EFFECT OF GLUCOSE AS STABILIZER OF ZNO AND CDO NANOPARTICLES ON THE MORPHOLOGY AND OPTICAL PROPERTIES

Nobathembu Faleni[1] & Makwena Justice Moloto[2*]

[1)]Department of Chemical Technology, University of Johannesburg, P. O. Box 17011, Doornfontein, 2028, South Africa

[2)]Department of Chemistry, Vaal University of Technology, Private Bag X021, Vanderbijlpark, 1900, South Africa

*Author for Corresponding : 2716 9509207 Fax: +27867563592

Email: makwenam@vut.ac.za

ABSTRACT

Most organic stabilizers for semiconductor nanoparticles used such as hexadecylamine, troctylphosphine oxide, alkylpyridine, organic thiols, oleic acids etc. are water insoluble and not biocompatible. Zinc and cadmium oxide nanoparticles give significant stability under the influence of any type of stabilizer. Glucose is a sugar molecule with both water solubility and biocompatibility and is used as capping for the CdO and ZnO nanoparticles. The synthesis of the nanoparticles was carried out in an alcoholic medium The amount of glucose is varied from 0.25 g to 1.00 g to study its influence on the morphologies and optical properties of the zinc and cadmium oxide nanoparticles. The morphologies of the nanoparticles were characterized by TEM images and the optical properties were analysed using UV-Visible spectrophotometry and photoluminescence, which shows the general blue shift in their absorption features and red shifts of the emission maxima. The use of glucose as stabilizer for nanoparticles provide route for direct synthesis of semiconductor nanoparticles especially at lower glucose amount to avoid its crystallinity obscuring the particles crystallinity.

Keywords: *Metal oxides, glucose-capped, zinc and cadmium oxide nanoparticles.*

1. INTRODUCTION

Semiconductor nanocrystals have been of interest in research and technical applications, with respect of its size-dependent optical and electronic properties [1-3]. Metal oxides play a very important role in many areas of chemistry, physics and materials science [4-9]. Generally metal elements form very large diversity of compounds with various stoichiometry [10] and can form a number of structural geometries with electronic structure that can display metallic, insulator or semiconductor character. The band gaps of metal oxides, ZnO (3.3 eV) and CdO (2.3. eV) makes them desirable for the applications relating to quantum mechanics [11], leading a role in various applications in piezoelectric transducers, light-emitting devices [12], photonic crystals [13], nanoelectronics [14], transparent UV protection and conductive films, chemical sensors and biological (drug delivery, bio-imaging, etc) systems [15-17]. Several synthetic methods have been employed to fabricate nanostructured metal oxides such as mechanochemical processing [18], metal alkoxide hydrolysis [19], hydrothermal [20] and nonhydrolytic sol-gel reaction process [21, 22].

The synthesis of ZnO and CdO nanoparticles by thermal decomposition is one of the most common methods to produce stable monodisperse suspensions with the ability of self-assembly. Nucleation occurs when the metal precursor is added into a heated solution in the presence of surfactant, while the growth state take place at a higher reaction temperature. Colloidal ZnO has been mostly produced in aqueous or alcoholic solutions by direct reaction of zinc compounds with bases in the presence of appropriate stabilizers [23-32]. A synthesis of nanoparticulate metal oxides is currently challenging and have limited usability when using organic compounds such as metal alkoxides as source of metals. When metal alkoxides are used as the precursors, the hydrolysis and polycondensation rate can be easily controlled by adjusting the reaction conditions [33-35]. Several methods have been reported for synthesis of metal oxide nanoparticles using metal inorganic salts as precursors [36-38], but most of these nanoparticles are poorly crystalline or exhibit broad particle size distribution. In the past years, a few studies on the quantum-confined effect and surface modifications on the electronic structure of the oxide nanoparticles have been published [39-40]. Reported results indicated that oxide nanoparticles may have different optical properties than the frequently studied II-VI semiconductor nanoparticles.

In this work, the conventional method has been used for the synthesis of metal oxide nanoparticle in which a base such as sodium or potassium hydroxide was used in the presence of metal salt to give metal oxide. This is also known as chemical capping, in which an organic molecule (glucose) is used to passivate the surface of the particles so that the particles do not agglomerate or ripen to form larger particles. This ensures that the nanoparticles

synthesized using different amounts of capping yields stable nanoparticles with uniform size distribution. The metal oxide nanoparticles were characterized for their optical properties and morphological features with varying amounts of capping agent. The properties of the metal oxides prepared depend on the size and structure of the particles, which are affected strongly by the synthetic processes and also control their widely varying optoelectronic and chemical properties [41].

2. EXPERIMENTAL DETAILS

2.1. Chemical reagents

The oxides of zinc and cadmium were synthesized using hydrated salts of zinc and cadmium chloride ($ZnCl_2$ and $CdCl_2{\cdot}H_2O$), methanol, sodium hydroxide, glucose which were purchased from Sigma Aldrich and used as obtained.

2.2 UV-visible and FT-IR spectroscopic measurements

The absorption spectra of ZnO and CdO were taken using a Analytikjena SPECORD 50 UV-visible spectrophotometer and the emission spectra were recorded on a LS 45 Perkin-Elmer fluorimeter with a Xenon lamp at room temperature using methanol as a solvent in a 1-cm pathlength quartz cuvette. Surface interaction of glucose on the nanoparticles of all samples was characterized using FT-IR Perkin Elmer 100 spectrometer. Measurements were performed with manually placing the solid sample on a diamond tip and pressed for analyses.

2.3 Electron Microscopy

The transmission Electron Microscopy (TEM) and High Resolution TEM images were obtained using a JEM -2100 JEOL electron microscope. The samples were prepared by placing a drop of a dilute solution of sample in methanol on a copper grid. The samples were allowed to dry completely at room temperature.

2.4 X-Ray Diffraction

X-Ray diffraction (XRD) patterns on powdered samples were measured on Phillips X'Pert materials research diffractometer using secondary graphite monochromated Cu Kα radiation (λ=1.54060 Å) at 40kV/50 mA. Measurements were taken using a glancing angle of incidence detector at an angle of 2º, for 2θ values over 20º-70º in steps of 0.05º with a scan speed of 0.05º $2\theta.s^{-1}$.

2.5 Synthesis of Zinc and Cadmium oxide nanoparticles

Zinc and cadmium oxide nanoparticles were synthesized using zinc chloride ($ZnCl_2$) and cadmium chloride ($CdCl_2.H_2O$), methanol (CH_3OH), sodium hydroxide (0.10 M) and glucose. The solutions were prepared in methanol (50 mL). To prepare 0.10 M solution, sodium hydroxide pellets were dissolved and in 20 ml methanol stirred for 20 minutes at room temperature. Amounts of glucose were varied from 1.00 g, 0.50 g and 0.25 g for each experiment was added into the prepared solution stirring and continued further for 40 minutes. Zinc chloride (0.10 M in 20 ml methanol) and was slowly added to this solution and stirred for 2 hours. The precipitate obtained was washed with methanol and separated by centrifuge and dried to get ZnO nanoparticles in solid form. The synthesis for cadmium oxide nanoparticles was carried out in a similar way.

3. RESULTS AND DISCUSSION

UV-Visible and fluorescence spectroscopy are powerful non-destructive techniques to explore the optical properties of semiconducting nanoparticles. The optical properties of glucose capped ZnO and CdO nanoparticles have been analyzed with methanol as a solvent. The absorption spectra of glucose capped ZnO and CdO in methanol solution in the UV range are presented in Fig. 1 and 3.

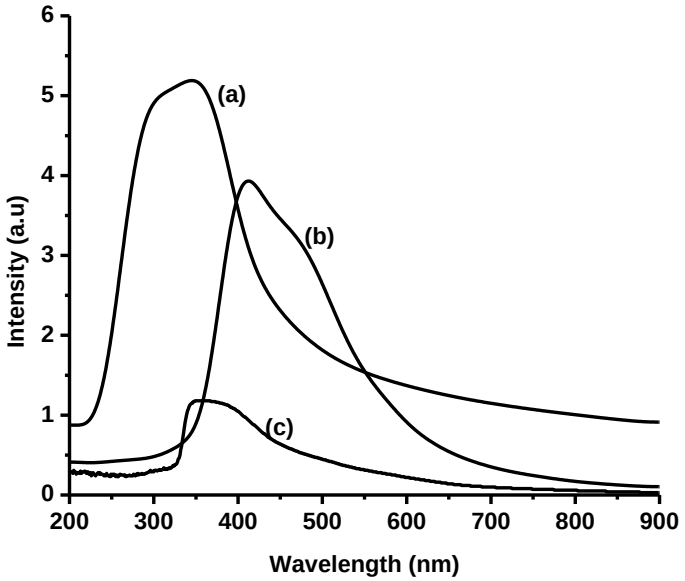

Figure 1: Absorption spectra of ZnO nanoparticles at different glucose amounts 1.00 g (a), 0.50 g (b) and 0.25 g (c).

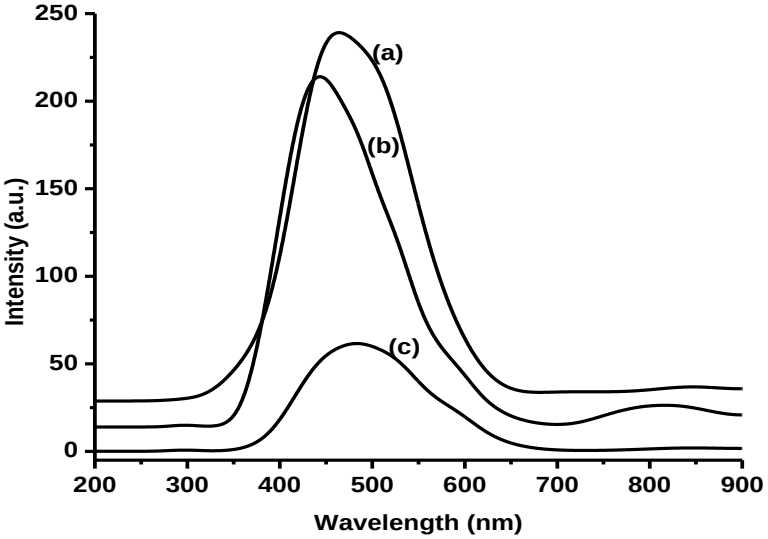

Figure 2: Emission spectra of glucose capped ZnO nanoparticles prepared using different amounts of glucose 1.00 g (a), 0.50 g (b) and (c) 0.25 g (c).

The glucose capped ZnO nanoparticles reveal absorption band edges at 417, 402 and 362 nm for amounts of 1.00 g, 0.50 g and 0.25 g, respectively, which shows red shifts in relation to the bulk, at high glucose amounts and that correlates with the change in the shapes. Fig. 2 illustrates room-temperature photoluminescence (PL) spectra of glucose capped ZnO nanoparticles. This indicate that the observed emission is intrinsic to glucose capped ZnO and red-shifted in relation to the absorption band edges. Glucose capped CdO nanoparticles (Fig. 3) gave absorption edges of 488, 482 and 468 nm for 1.00 g, 0.50 g and 0.25 g respectively, and are blue shifted in relation to the bulk band gap (bulk CdO, 538 nm). The PL spectra gave emissions at 518, 493 and 437 nm and are red shifted in comparison to the absorption band edges (Fig. 4). The blue shift in the excitation absorption reflects the correspondingly gradual removal of the initial trap and surface states during the crystallization process of nanoparticles.

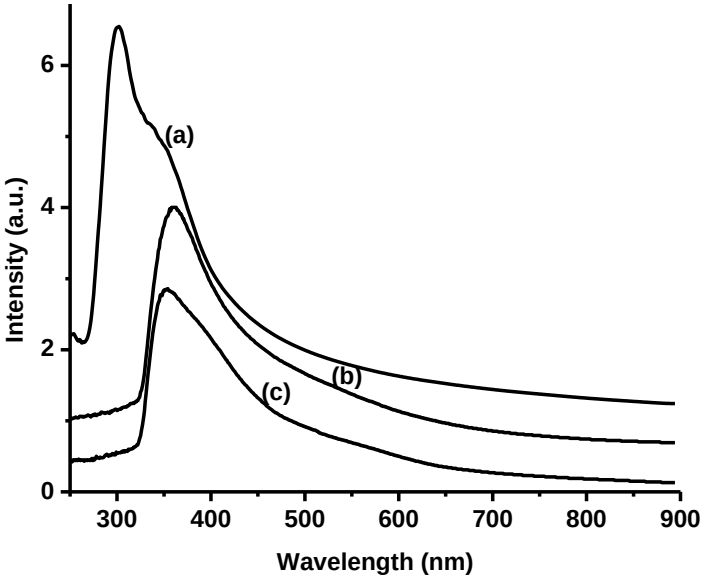

Figure 3: Absorption spectra of glucose capped CdO nanoparticles prepared using different amounts of glucose, 1.00 g (a), 0.50 g (b) and 0.25 g (c).

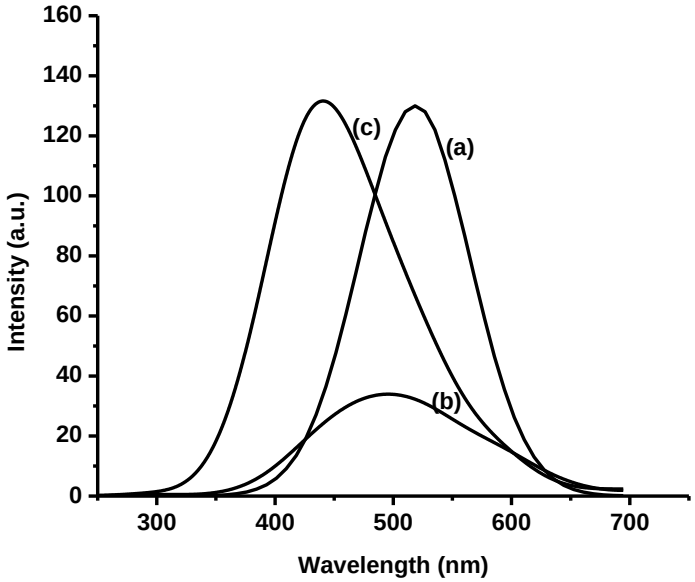

Figure 4: Emission spectra of glucose capped CdO nanoparticles prepared using different amounts of glucose 1.00 g (a), 0.50 g (b) and 0.25 g (c).

The morphology of glucose capped ZnO and CdO nanoparticles was examined by TEM and HMTEM (Fig. 5 and 6). Fig. 5 for glucose capped ZnO nanoparticles shows TEM and HMTEM images of the as-obtained nanocrystals from nanorods to spherical shapes. The particle size distribution of ZnO nanoparticles for the amounts, 1.00 g, 0.50 g and 0.25 g was determined to give rods with an average length of 80 nm, spheres of 4.2 – 4.9 nm and 6.0 – 8.0 nm, respectively.

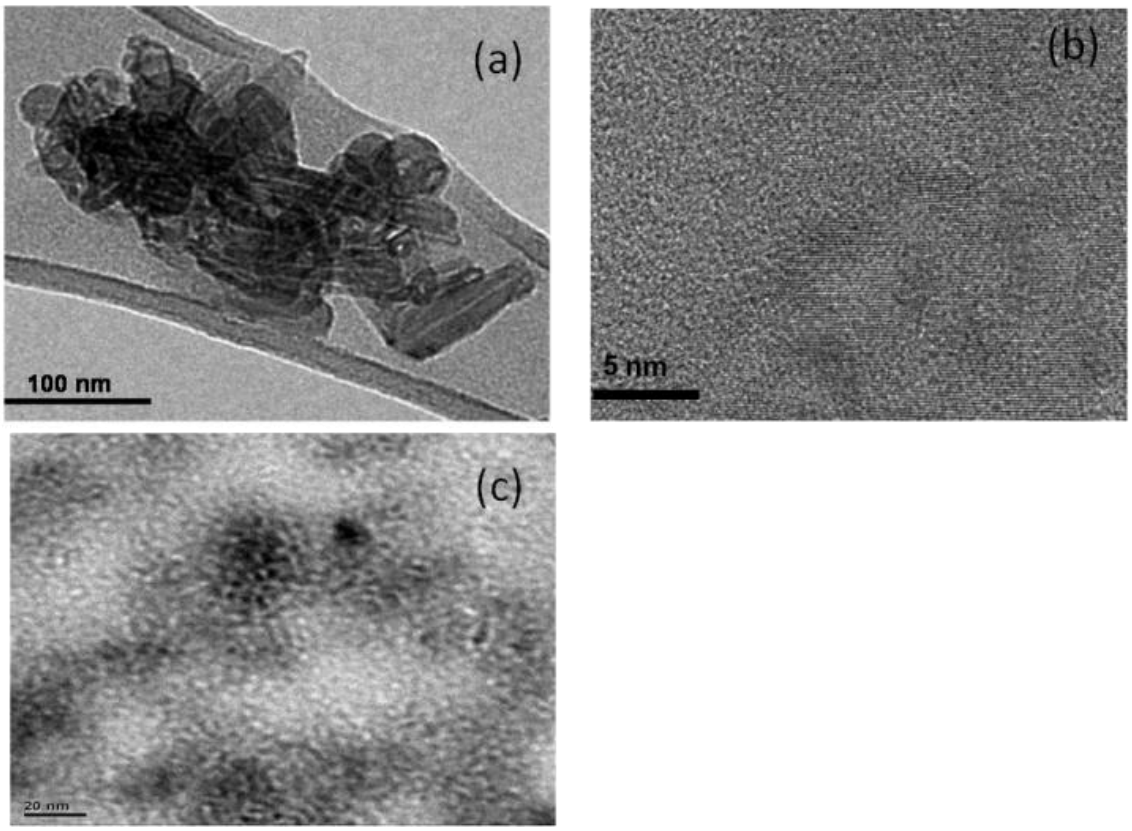

Figure 5: TEM images of glucose capped ZnO nanoparticles prepared using 1.00 g (a), 0.50 g (b) (HMTEM) and 0.25 g (c).

Lower concentration (0.25 g of glucose) gave larger particle sizes as compared to intermediate concentration (0.50 g of glucose) with smaller particle size for spherical shape. The highest concentration (1.00 g of glucose) gave rod shaped particles, which can be attributed to more glucose molecules on the surface of the particles from nucleation to growth combined with the structure of glucose molecule with OH groups. The capping agent provides protective organic shell to particles to prevent nanoparticles from aggregating in solution. The higher capping agent concentration (1.00 g glucose) promotes the formation of fewer, larger nuclei and, thus larger nanocrystals particle sizes. It also allows nanocrystals to be chemically manipulated like large molecules with solubility and reactivity determined by the identity of the surface ligands. It has been reported that varying the capping agent or ratio of the capping agent to precursor has changed particle morphology in a number of systems, due to varying ability to stabilize certain planes [42-44]. The crystal morphology is determined by the relative growth rates of the crystal planes, which can differ greatly due to differences in surface free energies [45, 46]. O'Brien and co-workers reported the synthesis of zinc oxide nanorods through nonhydrolytic method with a high degree of crystallinity and a narrow size distribution [47]. The particle size distribution showed different particle sizes for nanorods of 1,00 g glucose from 89 - 155 nm in length, nanospheres of 18 – 23 nm for 0.50 g glucose and 2.3 - 5.5 nm for 0.25 g glucose capped CdO nanoparticles. Fig. 6c shows TEM and high magnification TEM images for spherical particles of CdO nanoparticles with sizes ranging from small particles 2.0 – 5.0 nm and larger ones of 35 – 45 nm in diameters. At higher magnification lattice planes are observed indicating the high crystallinity of the particles prepared especially at 0.50 and 0.25 g of glucose (Fig. 6b and c).

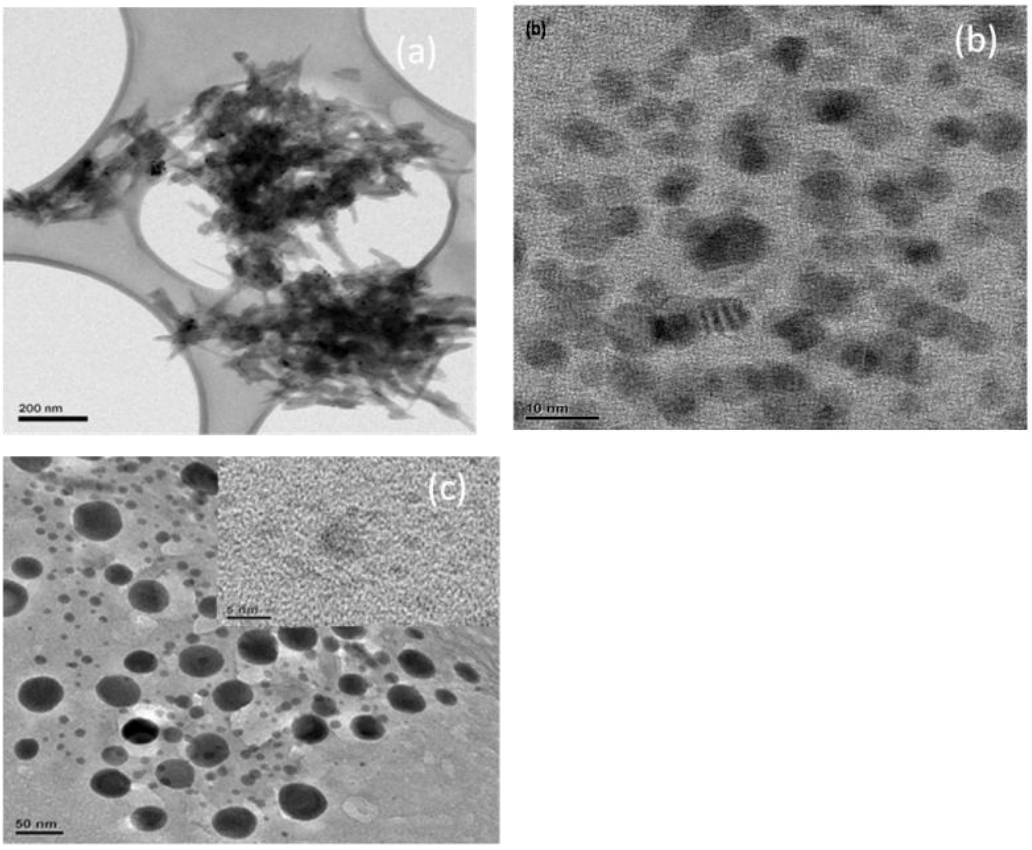

Figure 6: TEM images of (a) 1.00 g, (b) 0.50 g and (c) 0.25 g glucose- capped CdO nanoparticles.

The coordination of the surfactant molecules glucose on the surface of the nanoparticles (ZnO and CdO) prepared were characterized using Fourier Transform Infra-red (FTIR). The organic molecules in the synthesis of nanoparticles are to overcome the high surface energy and to stabilize their thermodynamically unfavourable state. These stabilizing agents control nucleation, growth and are able to bind on the surface of the crystals and stabilize them against aggregation. The surface chemistry of ZnO nanoparticles has been studied in which the growing rods showed similar features with nanodots, in which acetate groups were strongly chemisorbed to ZnO surfaces in ethanol, and instead of surface hydroxyl termination, there is a measurable presence of adsorbed ethanol solvent [48]. Fig. 7 and 8 shows FT-IR spectrum of glucose capped ZnO and CdO nanoparticles.

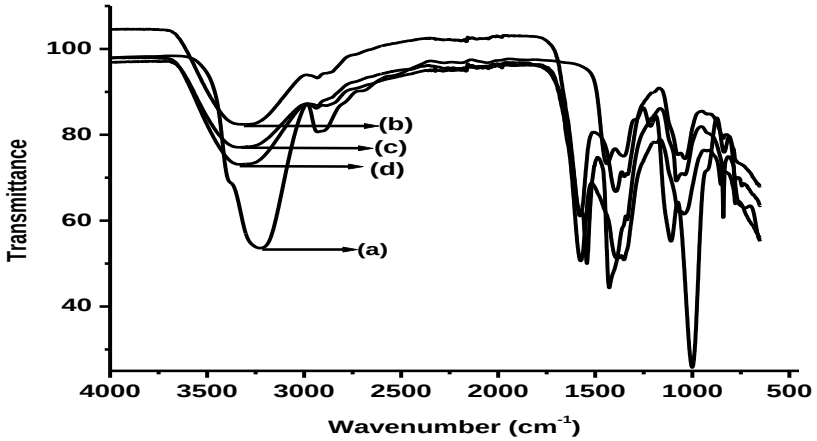

Figure 7: FT-IR spectrum of glucose ZnO nanoparticles prepared using 1.00 g (b), 0.50 g (c), 0.25 g (d) and free glucose (a).

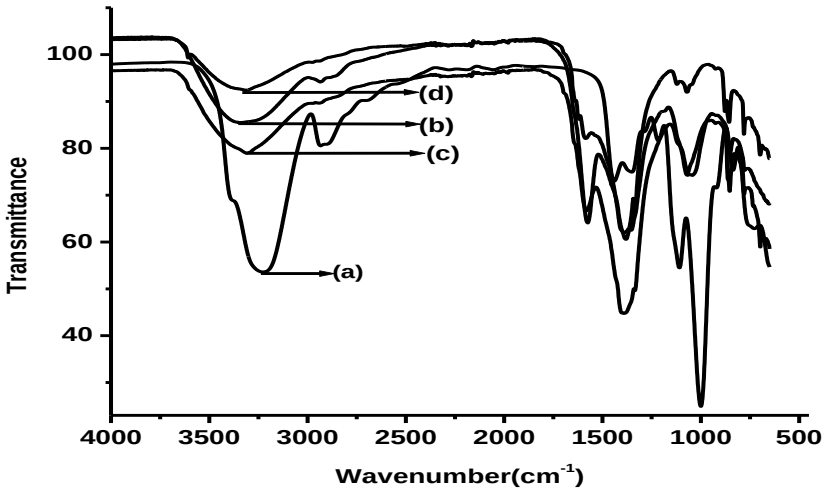

Figure 8: FT-IR spectra of glucose capped CdO nanoparticles prepared using 1.00 g (b), 0.50 g (c), 0.25 g (d) and free glucose (a).

The glucose capped ZnO nanoparticles showed peaks at 3342 cm^{-1} for O-H broad bands and appears at lower wavenumbers for glucose only 3246 cm^{-1}. It has been found the coupling of glucose and glucose capped ZnO spectrums appearance of peaks at 1442 and 1014 cm^{-1} for C-H bands. The intensity at 1572 cm^{-1} is attributed to C-O band and at 835 cm^{-1} Zn-O band for glucose capped ZnO indicating the interaction of glucose and zinc oxide nanoparticles. This indicated that the glucose capping has been introduced onto the nanoparticles surface. Fig. 8 shows characteristic broad bands at 33342 cm^{-1} for O-H band and at lower wavenumbers for glucose only of 3246 cm^{-1}. At 1394 and 1014 cm^{-1} indicates the C-H bands and 848 cm^{-1} showed characteristic band of Cd-O bond. Fig. 9 (a-c) shows typical XRD pattern of glucose capped ZnO diffraction peaks indexed to hexagonal phase. The diffraction peaks of as synthesised glucose capped CdO in Fig 10 (a-c) were indexed to crystalline cubic structure cadmium oxide along with (*) hexagonal phase. The solvothermal method was utilised to prepare single-crystalline cadmium oxide (CdO) micro-octahedron, polycrystalline CdO nanowires and cadmium hydroxide ($Cd(OH)_2$) nanorods by varying the amount of NaOH and synthesis temperature. The synthesis of CdO with an increase in a precursor concentration of sodium hydroxide (1 - 4 g) can lead to formation of mixed phases of cubic along with hexagonal phases [48]. All XRD patterns show obvious size-broadening effects, due to small crystallite sizes. The smaller particles diffracted the X-ray weakly compared to bigger ones and show broader peaks. The relative intensity of the peaks in the XRD spectra of the spherical nanoparticles matches the bulk, confirming the formation of wurzite ZnO nanocrystals [49,50].

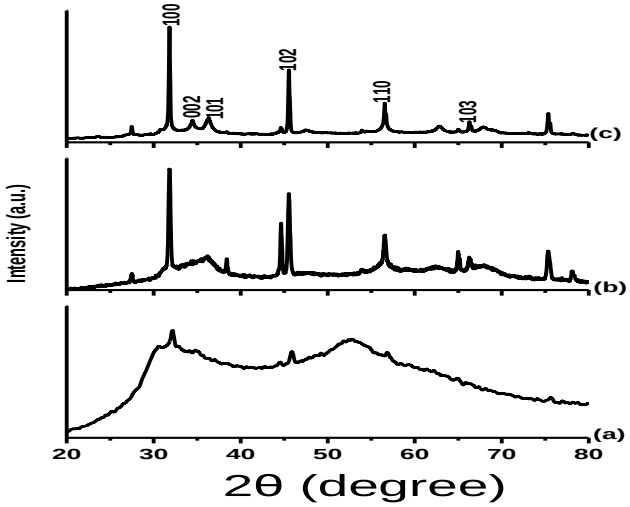

Figure 9: XRD spectra of glucose capped ZnO nanoparticles prepared using 1.00 g (a), 0.50 g (b) and 0.25 g (c) of glucose.

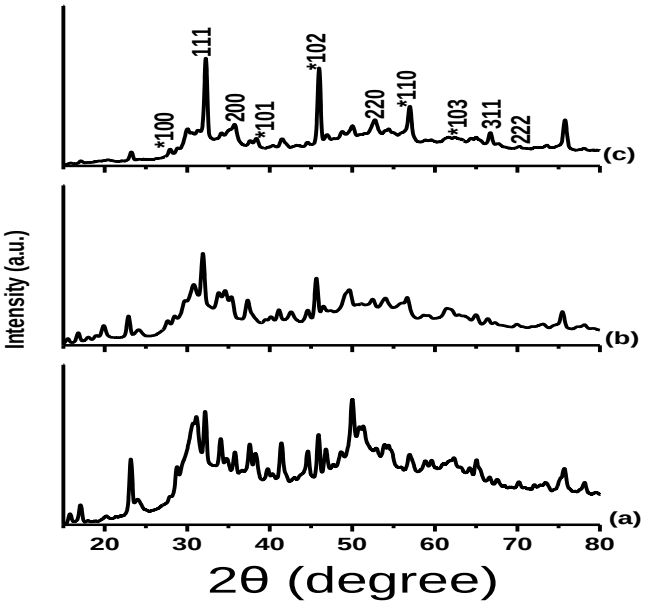

Figure 10: XRD spectra of glucose capped CdO nanoparticles prepared using 1.00 g (a), 0.50 g (b) and 0.25 g (c) of glucose.

4. CONCLUSIONS

The variation of glucose at 0.25 to 1.00 g affects the ZnO nanoparticles morphology and hence the red shifts at higher glucose amounts, 1.00 and 0.50 g of glucose. CdO nanoparticles show no variation in optical properties and morphology except particle size increases with increase in glucose amounts. The nanoparticles prepared showed different morphology from nanorods at 1.00 g to nanospheres at concentrations of 0.50 g and 0.25 g.

5. ACKNOWLEDGEMENTS

The authors would like to thank the National Research Foundation (NRF) in South Africa for funding, and the CSIR, and the University of Witwatersrand (Electron microscope unit) and University of Johannesburg which provided the laboratory space for the work.

6. REFERENCES

[1]. A. P. Alivisatos, *Science* **27**, 1933, (1996**)**.
[2]. S. Coe, W. K. Woo, M. Bawendi, V. Bulovic, *Nature* **420**, 800, (2002).
[3]. M. Bruchez, M. Moronne, P. Gin, S. Weiss, A. P. Alivisatos, *Science* **281**, 2013, (1998).
[4]. C. Noguera, *Physics and Chemistry at Oxide Surfaces*, Cambridge University Press: Cambridge, UK (1996).
[5]. H. H. Kung, *Transition Metal Oxides: Surface Chemistry and Catalysis*; Elsevier: Amsterdam (1989).
[6]. V. E. Henrich, P. A. Cox, *The Surface of Metal Oxides*; Cambridge University Press: Cambridge, UK (1994).
[7]. F. Wells, *Structural Inorganic Chemistry, 6th ed*; Oxford University Press: New York (1987).
[8]. J. A. Rodriguez, M. Fernández-Garcia (Eds.) *Synthesis, Properties and Applications of Oxide Nanoparticles*. Whiley: New Jersey (2007).
[9]. M. Fernández-Garcia, A. Martinez-Arias, J.C. Rodriguez, J. A. *Chem. Rev.* **104** (2004), 4063, (2004).
[10]. R. W. G. Wyckoff, *Crystal Structures, 2nd ed;* Wiley: New York (1964).
[11]. Prokes, K. L. Wang, *Mater. Res. Sci. Bull* **24**, 13, (1999).
[12]. J. Hu, T. W. Odom, C. M. Lieber, *Acc.Chem.Res.* **32**, 435, (1999).
[13]. S. Nakamura, *Science* **281**, 956, (1998).
[14]. C. A. Mirkin, *Science* **286**, 2095, (1999).
[15]. A. Mendoza-Galviain, C.Trejo-Cruz, J. Lee, D. Bhattacharya, J. Metson, P. J. Evans, U. Pala,*J. Appl. Phy.* **99**, 14306, (2006).
[16]. Honma, S. Hirakowa, K. Yamada, J. M. Bae, *Solid State Ionics* **118**, 29, (1999).

[17]. T. S. PhelyBobin, R. J. Muisener, J .T. Koberstein, F. Papadinmitrakopoulos, *Synth.Met*. **116**, 439, (2001).
[18]. P. G. McCormick, T. Tsuzuki, J. S. Robinson, J. Ding, *Adv. Mater*. **13**, 1008, (2001).
[19]. H. Kominami, M. Kohno, Y. Takada, M. Inoue, T. Inui, Y. Kera, *Ind. Eng. Chem. Res.*, **38**, 3925, (1999).
[20]. K. Okuyama, Y. Kousaka, N. Tohge, S. Yamamoto, J. J. Wu, R. C. Flagan, J. H. Seinfeld, *AIChEJ*. **32** (1986), 2010.
[21]. J. Joo, T. Yu, Y.W. Kim, H. M. Park, F. Wu, J. Z. Zhang, T. Hyeon, *J. Am. Chem. Soc.*, **125** (2003), 6553.
[22]. J. Tang, J. Fabbri, R. D. Robinson, Y. Zhu, I. P. Herman, M. L. Steiger-wald, L. E. Brus, *Chem. Mater*.,**16** (2004),1336.
[23]. U. Koch, A. Fojtik, H. Weller, A. Henglein, *Chem. Phys.Lett.* **122** (1985), 507.
[24]. D. W. Bahnemann, C. Kormann, M. R. Hoffmann, *J. Chem.* **91** (1987), 3789;
[25]. N. S. Pesika, K. J. Stebe, P. C. Searson, *Adv. Mater*. **15** (2003),1289;
[26]. L. Spanhel, M. A. Anderson, *J. Am. Chem. Soc*. **113** (1991), 2826.
[27]. S. Sakohara, M. Ishida, M. A. Anderson, *J. Phys. Chem.* B **102** (1998), 10169.
[28]. M. Haase, H. Weller, A. Henglein, *J. Phys. Chem*. **92** (1988), 482, (1998).
[29]. S. Sakora, L. D. Tickanen, M. A. Anderson, *J. Phys. Chem.* **96**, 11086, (1992).
[30]. A. Taubert, G. Wegner, *J. Mater. Chem.* **12**, 805, (2002).
[31]. P. Gerstel, R. C. Hoffmann, P. Lipowasky, L. P. H. Jeurgens, J. Bill, F. Aldinger, *Chem. Mater.* **18**, 179, (2006).
[32]. E .M. Wong, J. E. Bonevich, P. C. Searson, *J. Phys. Chem.* B, **102**, 7770, (1998).
[33]. T. Moritz, J. Reiss, K. Diesner, D. Su, A. Chemseddine, *J. Phys .Chem .B*. **101**, 8052, (1997).
[34]. T. He, D. Chen, X. Jiao, *Chem. Mater*. **16**, 737, (2004).
[35]. M. Aslam, L. Fu, M. Su, K. Vijayamohanan, V. P. Dravid, *J. Mater. Chem*. **14**, 1795, (2004).
[36]. M. Z.-C. Hu, M. T. Harris, C. H. Byers, *J. Colloid Interf Sci*. **198**, 87, (1998).
[37]. Y. Wang, C. Ma, X. Sun, H. Li, *Inorg. Chem. Commun*. **5**, 751, (2002).
[38]. Y. Jiang, Y. Wu, B. Xie, Y. Xie, Y. Qian, *Mater. Chem. Phys*. **74**, 234, (2002).
[39]. B. Zou, J. Lin, J. Xu, Q. Wei, L. Xiao, T. Li, *Phys. Low Dimens. Struct*. **5**, 173, (1996).
[40]. R. Aradjo, J. Butty, Peyghambarian, *N. Appl. Phys. Lett.* **68**, 584, (1996).
[41]. W. Stichert, F. Schüth, *Chem. Mater*. **10**, 2020, (1998).
[42]. T. Sau, C. Murphy, *J. Am. Chem. Soc*. **126**, 8648, (2004).
[43]. T. Herricks, J. Chen, Y. Xia, *Nano Lett*. **4**, 2367, (2004).
[44]. L. Manna, E. Scher, P. Alivasatos,J. Am. Chem. Soc. **122**, 12700, (2002).
[45]. C. Pacholski, A. Kornowski, H. Weller, *Angew Chem .Int. Ed.* **41,** 1188, (2002).
[46]. P. D. Cozzoli, A. Kornowski, H. Weller, *J. Am. Chem. Soc*. **125**, 14539, (2003).
[47]. .M. Yin, Y. Y. Gu, I. L. Kuskovsky, T. Andelman, Y. Zhu, G. F. Neumark, S. O'Brien, *J. Am. Chem. Soc.* **125**, 15981, (2003).
[48]. T. Ghoshal, S. Biswas, P. M. G. Nambissan, G. Majumdar, S. K. De, *Crystal Growth and Design*, **9**, 1287, (2009).
[49]. L. Guo, S. Yang, C. Yang, P. Yu, J. Wang, W. Ge, G. K. L. Wong, Appl. *Phys. Lett*. **76**, 2901, (2000).
[50]. S. Cho, J. Ma, Y.Kim, Y.Su, G. K. L. Wong, J. B. Ketterson, *Appl. Phys.Lett*., **75**, 2761, (1999).